Electronic Supplementary Information (ESI) for

Partial-surface-passivation strategy for Transition-metal-based Copper-Gold Nanocage

Shoujie Liu,[‡ab] Xusheng Zheng,[‡a] Li Song,[a] Wei Liu,[a] Tao Yao,[a] Zhihu Sun,[a] Yue Lin,[c] Shiqiang Wei,*[a]*

[a]National Synchrotron Radiation Laboratory, University of Science and Technology of China, Hefei 230029, P. R. China
[b]College of Chemistry and Materials Science, Anhui Normal University, Wuhu 241000, P. R. China
[c]Hefei National Laboratory for Physical Sciences at the Microscale, University of Science and Technology of China, Hefei 230026, P. R. China

[‡]These authors contributed equally.

*yaot@ustc.edu.cn; sqwei@ustc.edu.cn

Experimental

Sample synthesis*:* In a typical synthesis, 1 mmol copper(II) acetylacetonate, 4 mL oleylamine, and 10 mL trinoctylamine were prepared in a flask. The mixture was heated to 120 ºC in under magnetic stirring for 1 h and then slowly heated to 300 ºC at the rate of 2 ºC/min for two hours under ambient conditions. After it was cooled to 60 ºC, the color of the final colloidal solution turned a dark green-colored. It should be noted that the air ambient condition is intentionally used to oxidize the partial surface Cu atoms into CuO,[S1] which is critical to obtaining cage morphology in the next step. Then 4 ml of oleylamine containing 50 mg $HAuCl_4$ was rapidly injected into the above mixing solution under vigorous stirring, generating a black solution. The solution was reacted at 120 ºC for 30 min. The obtained nanocage was washed by 180 mL of ethanol and then was segregated three times at 9000 rpm for 3 min. For the synthesis of 3-nm solid Au nanoparticle, $HAuCl_4$ was mixed with oleic acid and oleylamine, and then was reacted at 180 ºC for 1h under nitrogen atmosphere. The solid Cu-Au nanoalloys of about 9 nm were prepared by the co-reduction of Copper acetate ($Cu(CH_3COO)$) and $HAuCl_4$ in oleic acid and oleamide at 180 ºC for 1h under nitrogen atmosphere. Then, the obtained particles were washed by ethanol several times and precipitated by centrifugation.

Characterizations*:* The transmission electron microscopy (TEM) images were obtained by a JEM-2010 TEM. The High-angle annular dark field (HAADF) imaging and STEM-energy dispersive spectroscopy (STEM-EDX) elemental mapping were carried out using a JEM-ARM200F TEM equipped with a spherical aberration (Cs) corrector (CEOS). The specimens were obtained by placing one or two drops of the colloidal cyclohexane solution of Cu-Au nanocage onto a thin amorphous carbon film-covered nickel microgrid and dried it in air at room temperature. Prior to the specimen preparation, the colloidal cyclohexane solutions were sonicated for 10 min to achieve a better particle dispersion on the nickle grid.

The depth-profiling X-ray photoelectron spectroscopy (XPS) measurements were carried on an Escalab 250 photoelectron spectrometer using low-dose argon plasma

etching and employing a monochromatic AlK_{α} X-ray source. Samples were mounted using double-sided adhesive tape and binding energies referenced to the C(1s) binding energy of adventitious carbon contamination which was taken to be 284.6 eV.

The inductively coupled plasma atomic emission spectroscopy (ICP-AES) result was recorded in a Perkin Elmer Optima 7300 DV ICP-OES instrument. X-ray diffraction (XRD) patterns were measured with a TTR-III X-ray diffractometer using Cu Kα line (λ = 1.5418 Å).

The XAFS spectra were collected at 1W1B station in BSRF (Beijing Synchrotron Radiation Facility, P.R. China) and 14W1 station in Shanghai Synchrotron Radiation Facility (SSRF). XAFS measurements at the Au L_3-edge and Cu-K edge were performed in transmission mode, using ionization chambers with optimized detecting gases to measure the radiation intensity. The analysis of EXAFS data are described in detail in the Supporting Information.

***Catalytic tests**:* Benzyl alcohol oxidation was carried out in a stainless steal autoclave with a nominal volume of 50 ml. Typically, 5 ml benzyl alcohol (BA), 20 ml deionized water and 12 mg catalysts were mixed with 5 ml Na_2CO_3–$NaHCO_3$ buffer solution (pH 9). Before reaction, the autoclave was purged five times with O_2 and then the pressure was kept at 3 atm during the reaction. The reaction temperature is 80 ºC with stirring rate of 1200 rpm. After reaction for 2 h, the reaction mixture was cooled down to room temperature. The reaction products were extracted with ethyl acetate and then analyzed by a FID-equipped GC. The Turn-Over-Frequency (TOF) of the catalysts can be calculated as (mole of benzaldehyde conversion) / (mole of surface Au atoms of catalyst×reaction time).

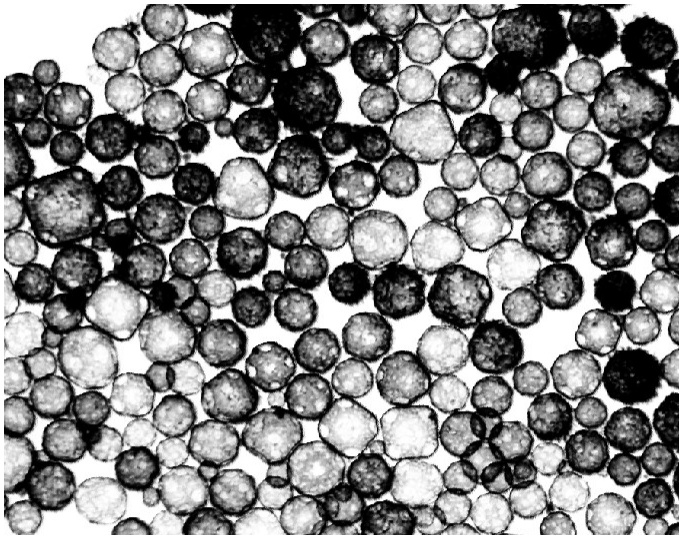

Figure S1. High-Angle Annular Bright Field (HAABF) STEM images of as-prepared Cu-Au alloy nanocage.

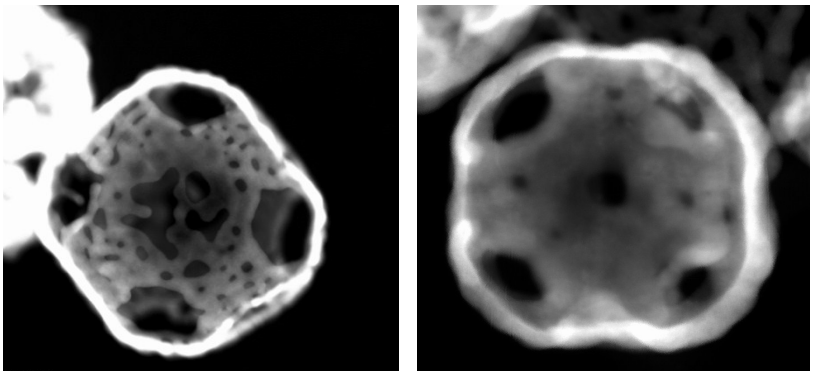

Figure S2. HADDF-STEM images of different individual Cu-Au alloy nanocages.

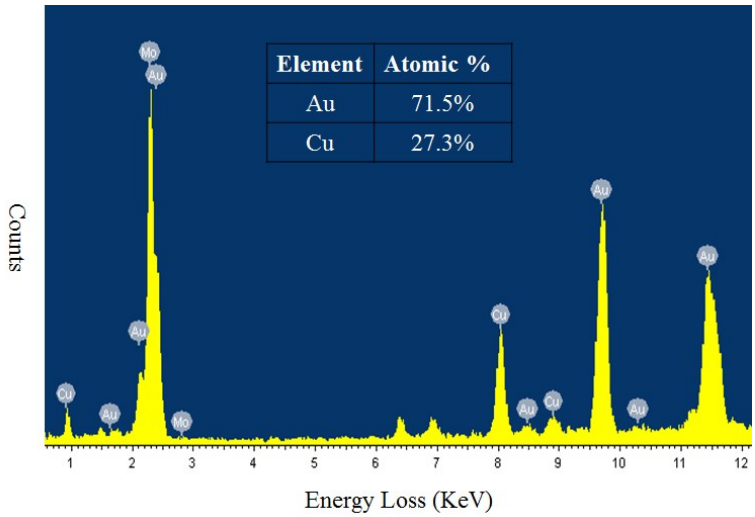

Figure S3. EDX spectrum of the as-prepared Cu-Au alloy nanocages. Mo came from the grid of STEM.

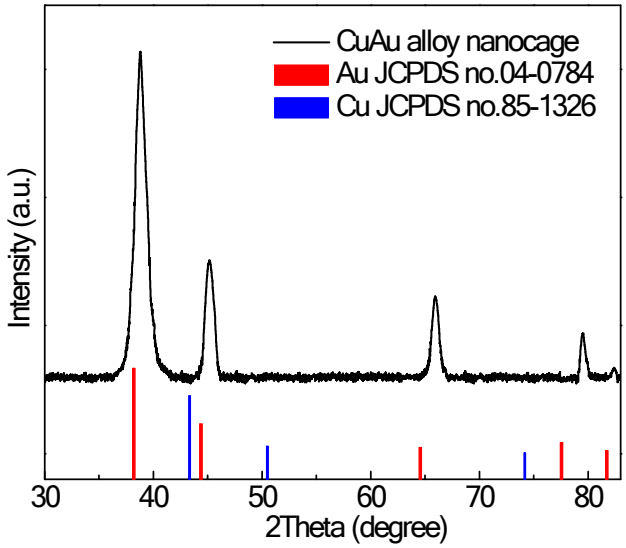

Figure S4. XRD pattern of the as-prepared Cu-Au alloy nanocages.

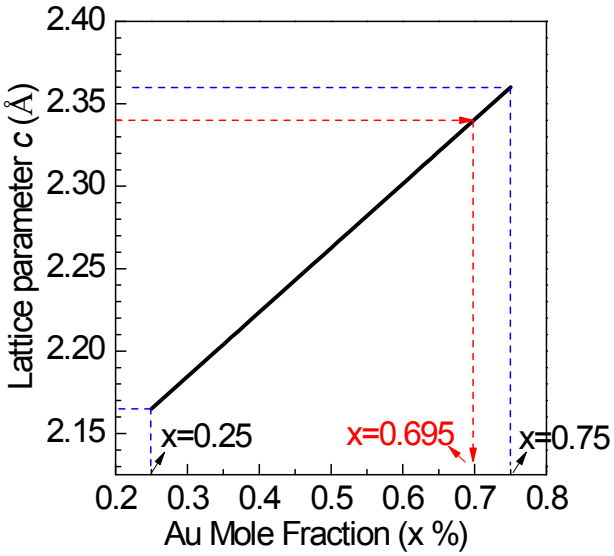

Figure S5. The dependence of the lattice parameters on the Au concentration is shown by choosing lattice parameters of Au_3Cu_1 (PDF#34-1302) and Au_1Cu_3 (PDF#35-1357). For our CuAu alloy nanocage, the calculated (111) interplanar spacing from XRD pattern is about 2.34 Å, corresponding to the Au concentration of 69.5%, which is in good agreement with that 71.5% obtained from ICP measurement.

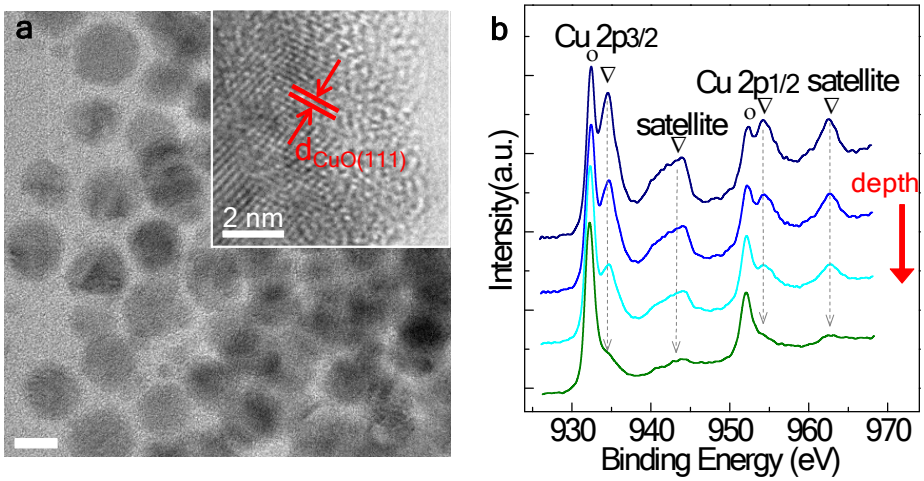

Figure S6. (a) Low-magnification TEM image of starting template nanoparticles. The inset shows a HRTEM image of the side in an individual nanoparticle; Scale bar, 50 nm. (b) The depth-profiling XPS spectra for the template nanoparticles using low-dose argon plasma etching. Each etch level was controlled at ca. 0.2 nm.

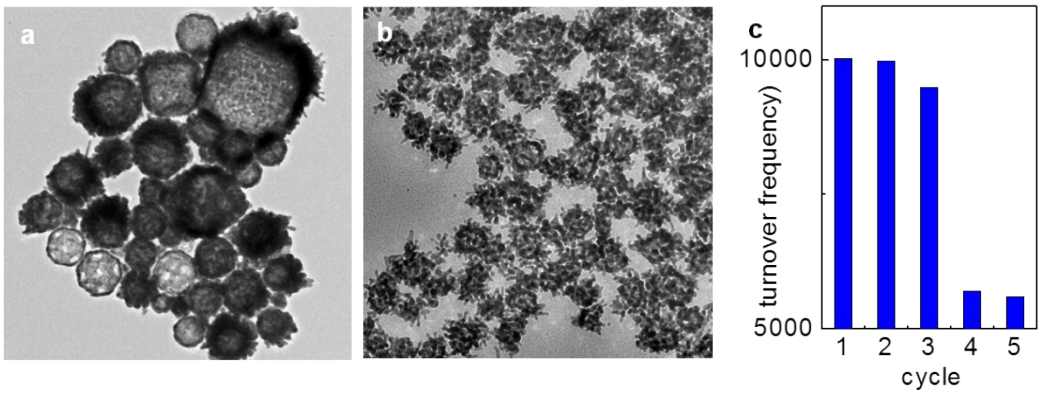

Figure S7. Re-usability of the catalyst. We have re-tested the catalytic performance of the sample for four times. It can be found that the catalytic efficiency of the CuAu nanocage maintains at a high level for the first three times. However, the TOF dramatically dropped to a quite low value of ca. 5700 h^{-1} for the fourth and fifth catalytic test of the sample. Furthermore, we have performed TEM measurement on the sample after the third test, and the image is shown as below. It can be found that the nanocage framework is collapsed, thus leading to the significant degrading of the performance.

EXAFS analysis: The acquired EXAFS data were processed according to the standard procedures using the ATHENA module implemented in the IFEFFIT software packages.[S2] The k^2-weighted EXAFS spectra were obtained by subtracting the post-edge background from the overall absorption and then normalizing with respect to the edge-jump step. Then, k^2-weighted χ(k) data in the k-space ranging from 2.2 to 13.3 $Å^{-1}$ were Fourier transformed to real (R) space using hanning windows (dk = 1.0 $Å^{-1}$) to separate the EXAFS contributions from different coordination shells. The quantitative information can be obtained by the least-squares curve fitting in the R space with a Fourier transform k space range of 3.0-12.0 $Å^{-1}$, using the module ARTEMIS of programs of IFEFFIT.[S3] The backscattering amplitude $F(k)$ and phase shift $\Phi(k)$ were calculated using FEFF8.0 code.[S4] The amplitude reduction factor S_0^2 of 0.90 and 0.85 obtained from fitting the bulk counterparts were fixed in fitting the subsequent Au and Cu edge data, respectively. Au-Cu scatting path with the coordination number and bond distance of N=12 and R=2.81 Å in an fcc-structured Au_3Cu intermetallic compound are used in the fit of Au-Cu shell. The structural parameters, such as the coordination number N, the interatomic distance R, and the Debye-Waller factor σ^2 were allowed to vary during the fitting process.

Table S1. Structural parameters extracted from quantitative EXAFS curve-fittings of Au L_3-edge data.

Time	Bond	R(Å)	N	$\sigma^2(10^{-3}Å^2)$
t1	Au-Au	2.87±0.02	10.9±0.4	7.4±0.5
t2	Au-Au	2.87±0.02	6.9±0.4	7.8±0.3
	Au-Cu (Alloy)	2.78±0.02	6.8±0.4	9.9±0.5
	Au-Au (Alloy)	2.78±0.02	4.5±0.4	9.0±0.5
t3	Au-Au	2.87±0.02	1.5±0.4	8.6±0.4
	Au-Cu (Alloy)	2.78±0.02	5.7±0.4	9.1±0.5
	Au-Au (Alloy)	2.79±0.02	5.8±0.4	8.6±0.5
t4	Au-Cu (Alloy)	2.78±0.02	3.3±0.4	7.6±0.5
	Au-Au (Alloy)	2.79±0.02	8.2±0.4	8.0±0.5

Table S2. Structural parameters extracted from quantitative EXAFS curve-fittings of Cu *K*-edge data. The template particles are denoted as 'TP'.

Time	Bond	*R*(Å)	*N*	$\sigma^2(10^{-3}Å^2)$
TP	Cu-Cu	2.55±0.02	11.8±0.4	7.3±0.5
	Cu-O	1.95±0.02	3.1±0.3	3.9±0.3
t1	Cu-Cu	2.55±0.02	9.5±0.4	7.8±0.5
	Cu-O	1.95±0.02	3.1±0.3	4.0±0.3
t2	Cu-Cu	2.55±0.02	8.9±0.4	8.2±0.5
	Cu-O	1.95±0.02	3.0±0.3	4.1±0.3
	Cu-Au (Alloy)	2.78±0.02	3.8±0.4	9.9±0.5
	Cu-Cu (Alloy)	2.78±0.02	5.1±0.4	9.6±0.5
t3	Cu-Cu	2.55±0.02	2.2±0.4	9.0±0.6
	Cu-O	1.95±0.02	3.0±0.3	4.4±0.3
	Cu-Au (Alloy)	2.79±0.02	5.1±0.4	9.9±0.5
	Cu-Cu (Alloy)	2.78±0.02	5.2±0.4	9.6±0.5
t4	Cu-O	1.95±0.02	1.8±0.3	4.4±0.3
	Cu-Au (Alloy)	2.79±0.02	7.6±0.4	9.6±0.5
	Cu-Cu (Alloy)	2.78±0.02	3.1±0.4	9.3±0.5

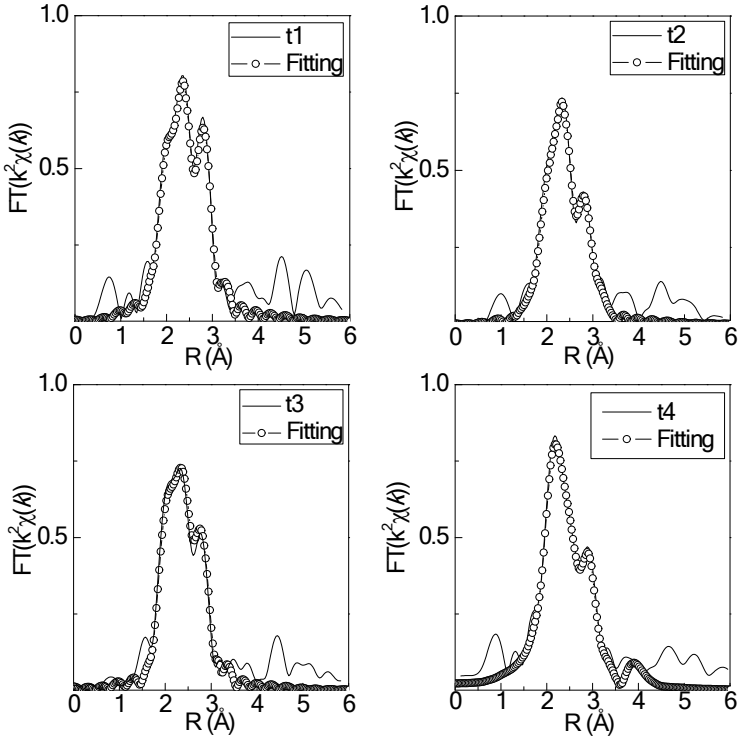

Figure S8. Au L-edge EXAFS curve-fitting results at different times of reaction.

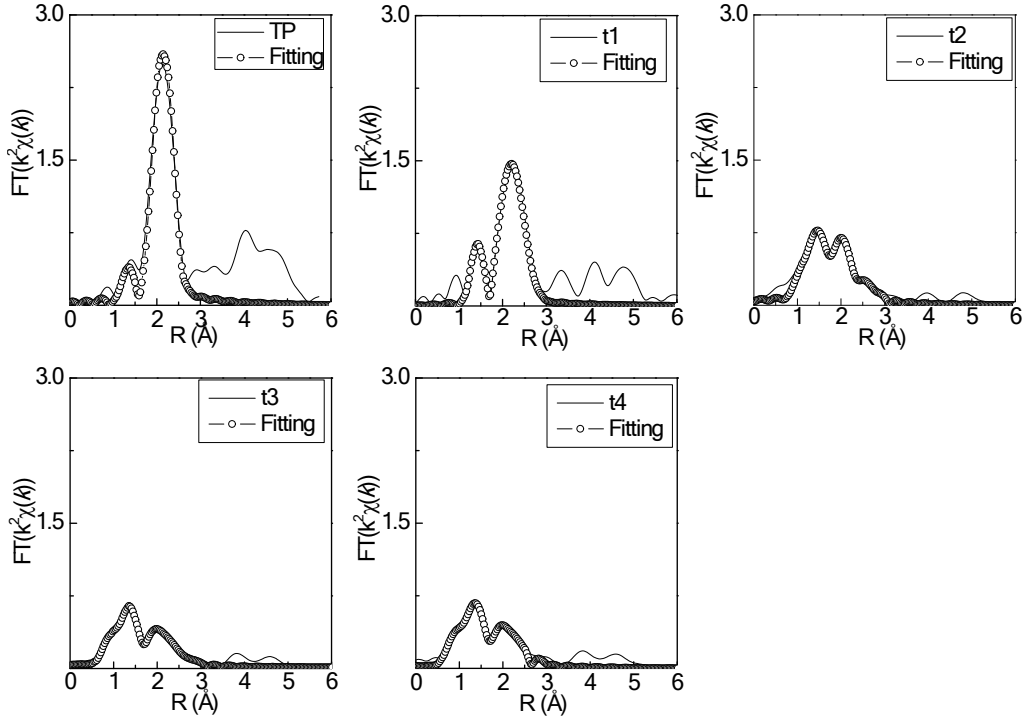

Figure S9. Cu K-edge EXAFS curve-fitting results at different times of reaction.

References

(S1) Hung, L. I.; Tsung, C. K.; Huang, W. Y.; Yang, P. D.; Room-Temperature Formation of Hollow Cu_2O Nanoparticles. *Adv. Mater.* **2010**, 22, 1910.

(S1) Newville, M. IFEFFIT : interactive XAFS analysis and FEFF fitting. *J. Synchrotron Rad.* **2001**, 8, 322.

(S2) Ravel, B.; Newville, M. ATHENA, ARTEMIS, HEPHAESTUS: data analysis for X-ray absorption spectroscopy using IFEFFIT. *J. Synchrotron Rad.* **2005**, 12, 537.

(S3) Ankudinov, A. L.; Ravel, B.; Rehr, J. J.; Conradson, S. D. Real-space multiple-scattering calculation and interpretation of x-ray-absorption near-edge structure. *Phys. Rev. B* **1998**, 58, 7565.